ChemPlusChem

A Multidisciplinary Journal Centering on Chemistry

Chemistry Europe

European Chemical Societies Publishing

Accepted Article

Title: A novel collagen aerogel with features relevant for topical biomedical applications

Authors: Miguel P. Batista, Baldur Schroeter, Naiara Fernández, Frédéric Bustos Gaspar, Maria do Rosário Bronze, Ana Rita Cruz Duarte, and Pavel Gurikov

To be cited as: *ChemPlusChem* **2024**, e202400122

Link to VoR: https://doi.org/10.1002/cplu.202400122

WILEY VCH

10.1002/cplu.202400122

WILEY VCH

RESEARCH ARTICLE

A Novel Collagen Aerogel With Relevant Features For Topical Biomedical Applications

Miguel P. Batista,[b,c] Baldur Schroeter,[a] Naiara Fernández,[b] Frédéric Bustos Gaspar,[b,d] Maria do Rosário Bronze,[b,d,e] Ana Rita Duarte,[c] and Pavel Gurikov*[a,f]

[a] Dr. B. Schroeter, Dr. P. Gurikov
Institute of Thermal Separation Processes
Hamburg University of Technology
Eißendorfer Str. 38, 21073 Hamburg, Germany
E-mail: pavel.gurikov@tuhh.de

[b] M. P. Batista, Dr. N. Fernández, Dr. F. B. Gaspar, Prof. Dr. M. R. Bronze
iBET, Instituto de Biologia Experimental e Tecnológica
Apartado 12, 2781-901, Oeiras, Portugal

[c] M. P. Batista, Prof. Dr. A. R. Duarte
LAQV-REQUIMTE, Departamento de Química, Faculdade de Ciências e Tecnologia,
Universidade Nova de Lisboa
2829-516, Caparica, Portugal

[d] Dr. F. B. Gaspar, Prof. Dr. M. R. Bronze
Instituto de Tecnologia Química e Biológica António Xavier
Universidade Nova de Lisboa
Av. da República, 2780-157, Oeiras, Portugal

[e] Prof. Dr. M. R. Bronze
Faculdade de Farmácia
Universidade de Lisboa
Avenida Professor Gama Pinto, 1649-003, Portugal

[e] Prof. Dr. M. R. Bronze
Faculdade de Farmácia
Universidade de Lisboa
Avenida Professor Gama Pinto, 1649-003, Portugal

Abstract: Collagen-based aerogels have great potential for topical biomedical applications. Collagen's natural affinity with skin, biodegradability, and gelling behavior are compelling properties to combine with the structural integrity of highly porous matrices in the dry form (aerogels). This work aimed to produce a novel collagen-based aerogel and to perform the material's solid-state and physicochemical characterization. Aerogels were obtained by performing different solvent exchange approaches of a collagen-gelled extract and drying the obtained alcogels with supercritical CO_2. The resulting aerogels showed a sponge-like structure with a relatively dense mesoporous network with a specific surface area of 201–203 m^2/g, a specific pore volume of 1.08–1.15 cm^3/g, and a mean pore radius of *ca*. 14.7 nm. Physicochemical characterization confirmed that the obtained aerogels are composed of pure collagen, and the aerogel production process does not impact protein tertiary structure. Finally, the material swelling behavior was assessed at various pH values (4, 7, and 10). Collagen aerogels presented a high water uptake capacity up to ~2700 wt.%, pH-dependent stability, and swelling behavior in aqueous media. The results suggest that this collagen aerogel could be a promising scaffold candidate for topical biomedical applications.

Introduction

Collagen, the predominant structural protein in the extracellular matrix of animal tissues, has gained substantial attention in the biomedical domain due to its biocompatibility, bioactivity, gelling behavior, and role in tissue regeneration [1]. Collagen is a fibrous protein that consists of three polypeptide chains intertwined into a triple helix. This triple helical structure imparts collagen with remarkable tensile strength, stability, and resistance to mechanical stress. This structural integrity makes collagen a valuable biomaterial and a key component of tissues like skin, tendons, and bones [2].

Collagen-based biomaterials are extensively used in tissue engineering and regenerative medicine. These biomaterials are mainly available in a hydrated gel state. However, drying can stabilize the shape of collagen materials, create pores with specific sizes and shapes, and extend the shelf life before usage. Furthermore, most methods for sterilizing collagen materials can only be employed when the materials are in a dry state. However, drying significantly alters the structure of the initial material. The originally expanded structure of collagen-gelled preparations changes as water is removed due to capillary forces [1,3]. In addition, drying processes often require precise temperature

control to preserve collagen's tertiary structure and mimic the native tissue environment. Any deviations in the collagen structure can compromise the biocompatibility and functionality of these biomaterials [2]. The conventional air-drying process can lead to undesirable outcomes such as thermal denaturation, shrinkage, pore closure, and even network collapse due to the strong surface tension of water [3]. Conversely, freeze-drying, involves removing water through the sublimation of frozen hydrogels. In the frozen state, ice crystals are formed within the gel network, causing expansion and distortion of the delicate structure of the wet gel. Supercritical CO_2 ($scCO_2$) drying is a viable option to circumvent these drawbacks, although it cannot be directly applicable to hydrogels due to the poor miscibility between CO_2 and water [4]. Since collagen gelation occurs in an aqueous medium, water must be substituted with an organic solvent before supercritical drying. Alcogels dried via the $scCO_2$ method result in aerogels, which are materials of a lightweight nature with high open porosity and remarkable physicochemical properties [5].

In recent years, aerogels have emerged as a versatile and promising biomaterials class, characterized by their low density and high specific surface area. They typically comprise a three-dimensional network of interconnected nanofibers, resulting in macro- to mesoporous structures, which might be shaped as monoliths, fibers, or particles of different sizes and sphericity [4,5]. The design and development of novel aerogels tailored for biomedical applications have garnered significant attention, with wound healing, tissue engineering, and drug delivery being the most attractive fields [6]. The high porosity of aerogels allows them to absorb and retain a significant amount of fluids, making them very appealing materials for wound dressings. Their outstanding absorption capacity can help maintain a moist wound environment, accelerating the healing process [7]. Moreover, aerogels can be excellent carriers for pharmaceutical compounds and antimicrobial agents due to their tailorable porosity and large surface area. They can be engineered to carry a high load of drugs that can be released based on specific stimuli, such as changes in pH or temperature, enabling the controlled and sustained release of drugs. [6,7].

Collagen aerogels represent an exciting innovation in topical biomedical applications, harnessing the unique properties of both collagen and aerogel materials. This synergistic combination of collagen's biocompatibility and regenerative capabilities with its remarkable porosity, mechanical tunability, and stability offers many advantages that make collagen aerogels a promising candidate for various biomedical uses. There are several published works on producing collagen aerogels [8–20]. Most of them present the production of porous collagen matrices by freeze-drying, wherein ice crystals are formed in the freezing process. As a result, the densification of primary nano-sized fibers occurs, forming macroporous solids (cryogels). As a result, materials of low specific surface area are obtained, lacking the typical characteristics of mesoporous aerogels. Thus, drying collagen gels by $scCO_2$-drying can potentially produce mesoporous collagen aerogels, which have only been scarcely reported so far. [8]. However, drying collagen gels with this technique can be a challenging process. The high temperature during supercritical drying may lead to thermal protein degradation. Collagen is sensitive to heat, and prolonged exposure to high temperatures can damage structural integrity and changes in functionality [3]. Furthermore, replacing water with an organic solvent miscible with $scCO_2$, is also a challenging step. Proteins are generally not directly soluble in organic solvents such as ethanol, typically used in the solvent exchange (SE) step. This work describes a pioneering approach to producing collagen aerogels using an extract developed in a previous work by the authors [21] as a collagen source. The extract comprises biocompatible marine collagen and the green extracting solvent, a natural deep eutectic solvent (NADES). The present study comprehensively explored the synthesis process, solid-state characterization, and the material's physicochemical characterization. After the aerogel production process, the collagen's structural integrity and swelling behavior were also evaluated, providing insights into its potential applications in the topical biomedical field.

Results and Discussion

In this work, we present for the first time a new aerogel entirely composed of collagen. After gelling the collagen-NADES extract obtained [21], ethanol was used for SE as a safer, lower-toxicity, and greener organic solvent compared to other conventional options. However, this solvent is also frequently used as a protein precipitation agent [4]. When trying to perform SE with our gels, with ethanol, a precipitated and impermeable collagen skin layer was obtained, making the interior of the gel almost inaccessible to ethanol (data not shown). This result impaired the use of ethanol as a solvent and other methodologies had to be developed. This indicates that indeed the SE of the collagen-NADES hydrogel is a critical and delicate step in the aerogel production process.

To better understand the influence of the solvent nature and exchange protocol, alcogels were produced with methanol (Table 2), directly changing with 100% solvent (direct SE) or by raising the solvent concentration in water mixtures of 25, 50, 75, and 100 vol% (stepwise SE). For the direct SE approach, the temperature influence was evaluated by running the SE process at 4 and -20 ºC (cryo SE). Temperatures higher than 4 ºC were not tested since collagen-NADES gel only remains self-supporting below *ca.* 4 ºC. The use of methanol allowed us to obtain collagen alcogels without the formation of a precipitated collagen layer. Alcogels obtained by direct, stepwise, and cryo SE were then dried by supercritical fluid technology, and the resulting materials were characterized via scanning electron microscopy (SEM) and nitrogen physisorption to elucidate morphology and textural properties.

10.1002/cplu.202400122

RESEARCH ARTICLE

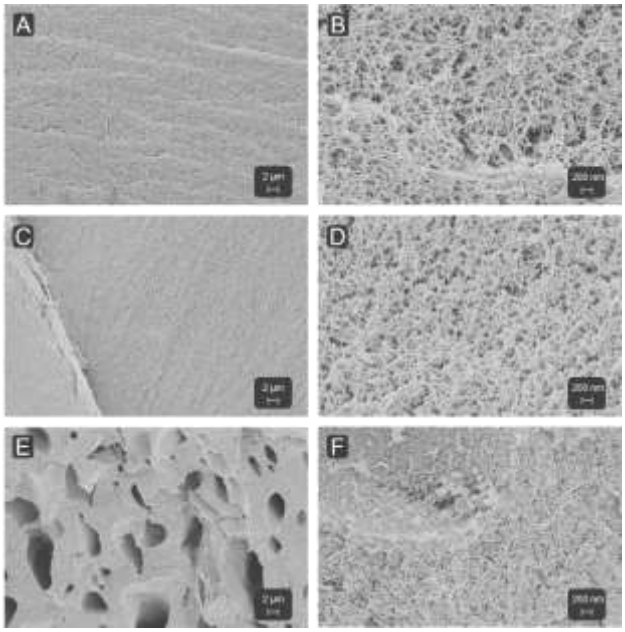

Figure 1. SEM micrographs of aerogels produced by SE with methanol: direct SE (A, B), stepwise SE (C, D), and cryo SE (E, F) at 5,000x (A, C, E) and 50,000x (B, D, F) magnification.

The materials prepared with cryo SE (Figure 1 E and F) presented a structure consisting of large macropores (pore diameter in the range of several µm) with dense areas between pores, while aerogels produced via SE at 4 ºC showed loose mesoporous structures with comparably high void volume (Figure 1 A, B, and C, D). Since the gel was frozen at -20 ºC in the cryo SE before adding methanol, a certain fraction of water in the hydrogel apparently formed ice crystals that resulted in macroporous voids. This morphology is not typical for aerogels [22] and somewhat resembles that of freeze-dried materials [9,11,14–20].

Both direct and stepwise SE at 4 ºC render aerogels with similar morphology (SEM micrographs in Figure 1 A, B, and C, D) indicating the efficacy of the $scCO_2$ drying in maintaining the structural integrity of the initial hydrogels. SEM micrographs at higher magnification (50,000x magnification; Figure 1 B and D) allowed us to verify that a similar network of interconnected nanofibers constitutes the aerogels obtained from direct and stepwise SE. This result was quantified via nitrogen physisorption, which showed no significant differences, between the processes in terms of isotherm shape (Figure 2 A), pore size distribution (Figure 2 B), specific surface area, and mesopore volume (Table 1), measured by Brunauer–Emmett–Teller (BET) and Barrett Joyner–Halenda (BJH) methods, respectively.

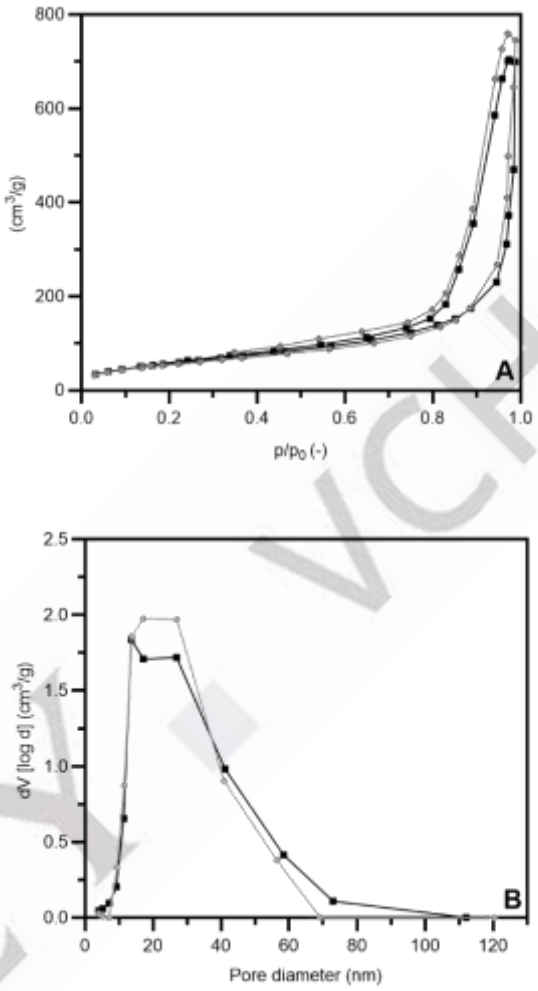

Figure 2. Isotherms (A) and corresponding pore size distributions (B) for samples produced via direct (—■—) and stepwise (--●--) solvent exchange with methanol at 4 ºC.

Table 1. BET surface area, BJH pore volume, and mean pore diameter of direct SE , cryo SE and stepwise SE aerogels.

Samples	Specific surface area (m^2/g)	Pore volume (cm^3/g)	Mean pore diameter (nm)
Direct SE	213	1.08	30.6
Cryo SE	-	-	-
Stepwise SE	201	1.15	27.9

Note: standard error of 5%

The samples showed a typical type IV isotherm of H3-like shape (Figure 2), which is indicative of systems consisting of meso- and small macropores, in agreement with qualitative assessment by SEM. Therefore, the corresponding pore size distributions are relatively broad and cover pore sizes in the whole mesoporous and the small macroporous ranges. Generally, values of specific surface area and mesopore volume are comparable with the

10.1002/cplu.202400122

corresponding values for different protein-based aerogels reported in the literature , [23–25]. Cryo SE textural values are not shown in Table 1 since the size of the pores in these samples was above the practical limit of the N_2 sorption methodology [26].

Since differences in the textural properties between direct and stepwise SE approaches are negligible, we suggest direct SE as a more efficient and straightforward process for producing collagen aerogels with the potential for future scale-up and industrial processes. The direct SE aerogel was therefore chosen to perform additional physical and chemical characterization to evaluate the impact of the aerogel production process on the collagen quality.

As mentioned above, the aerogels were prepared directly from a collagen-NADES extract obtained in a previous work developed by the authors [21]. During aerogel production, the SE step replaces all water in the collagen-NADES hydrogel with methanol (confirmed by density measurements). However, during this process, the constituent compounds of NADES (citric acid and xylitol) are extracted, and the gel becomes stiffer. To evaluate the collagen purity in the final aerogel, thermogravimetric analysis (TGA) was performed. Figure 3 compares the thermal behavior of the aerogel with two reference samples: (1) commercial standard of collagen and (2) starting collagen-NADES extract, which was dialyzed against distilled water to remove the NADES. TGA analysis allows the identification of potential contaminants by examining the sample's thermal decomposition profile. The thermograms in Figure 3 A present similar profiles, with the final mass percentage stabilizing at 30 %. The thermograms indicate a weight loss due to moisture evaporation from room temperature to 150 °C, and between 200 and 500 °C associated with collagen decomposition [21]. The slight differences between thermograms were further analyzed by DTGA (first derivate) curves (Figure 3 B). Regarding dry mass and maximum decomposition rate temperatures, the results indicate that the direct SE aerogel sample presents a 3-4 wt% difference to the commercial collagen standard and the dialyzed extract. This wt% difference could be due to the remaining NADES compounds not extracted in the SE step. However, the marginal presence of these compounds is not a critical point for potential topical biomedical applications since the NADES is composed of natural and biocompatible components.

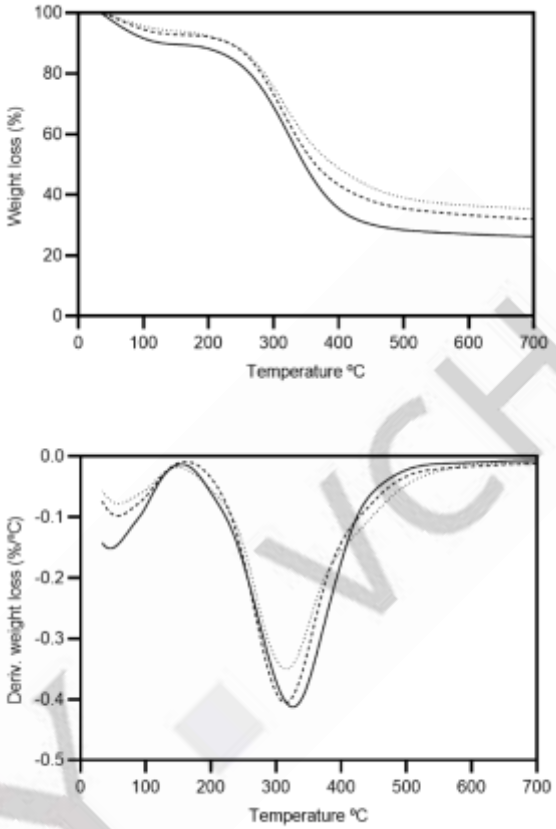

Figure 3. TGA (A) and DTGA (B) data of commercial Type I collagen from calf skin (—), dialyzed extracted collagen (----), and aerogel processed via direct SE (·····).

Figure 4 shows the sodium dodecyl sulphate-polyacrylamide gel electrophoresis (SDS-PAGE) band patterns of the commercial references, type I collagen from calf skin and gelatin from fish skin, dialyzed extracted collagen, and aerogel processed via direct SE. Commercial collagen presented the expected structure composed of two separate α-chains about 120 kDa and a beta component nearly 200 kDa, which is typical for Type I collagen. In contrast, the gelatin from fish skin showed dye retention down the lanes, typical of a hydrolyzed collagen format. In contrast, the fish skin gelatin showed dye retention down the lanes, typical of a hydrolyzed collagen format. Similar electrophoretic band patterns of the dialyzed collagen, collagen aerogel, and the commercial collagen standard (Figure 4, lanes 4, 5 and 2, respectively) were observed despite slight differences in α-chains molecular weight due to different collagen animal sources [27]. The similarity of bands' distribution suggests that both extracted collagen samples contain highly pure type I collagen and that the aerogel production process did not lead to collagen degradation.

10.1002/cplu.202400122

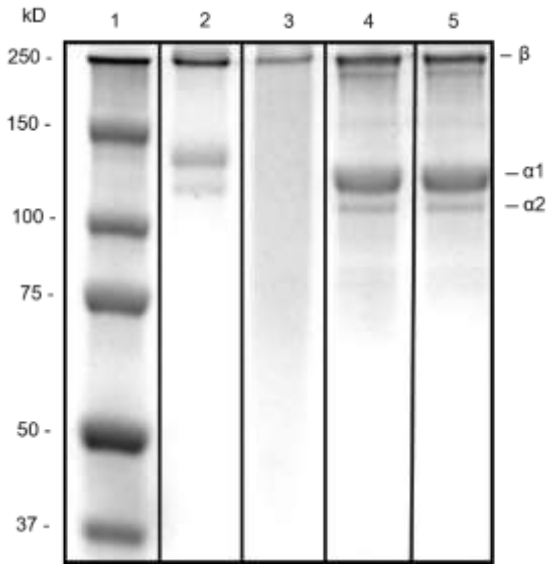

Figure 4. Electrophoretic profile (SDS-PAGE) of molecular weight standards (1); commercial type I collagen from calf skin (2), commercial gelatin from fish skin (3), dialyzed extracted collagen (4), and aerogel processed via direct SE (5).

The fourier-transform infrared (FTIR) spectra of the commercial references (commercial type I collagen from calf skin and gelatin from fish skin), extracted collagen aerogel, and dialyzed extracted collagen are exhibited in Figure 5 A. To determine if the triple helical collagen was present and maintained after the aerogel production process in the extracted collagen samples, spectral data based on Amide I and Amide II regions were interpreted in detail (Figure 5 B) and converted in the corresponding second derivative spectra presented in Figure 5 C (peaks in the opposite direction of Figure 5 A and B).

The overall spectra profiles present the typical collagen/gelatin molecular chain bands related to amide A, amide I, II, and III [28]. The peak for amide I, from the stretching vibrations of the carbonyl groups (C=O) in proteins, is observed at ~1650 cm^{-1}. The second derivative spectra of the commercial collagen in the Amide I region revealed two major absorption peaks at 1656 cm^{-1} and 1625 cm^{-1}. The Amide I peaks had previously been described, suggesting that a high-frequency absorption peak at about 1660 cm^{-1} represents ordered hydrogen bonds between the molecules present in the collagen tertiary structure, and a lower band nearly 1630 cm^{-1} attributed to water-bound peptides usually associated to denatured collagen [29,30]. The commercial gelatin from fish skin had a single peak at 1629 cm^{-1}, generally associated with the absence of a triple helix. Dialyzed collagen and aerogel processed via direct SE had two peaks at 1657 cm^{-1} and 1628 cm^{-1} in the second derivative spectra of the Amide I region. Unlike the gelatin sample, the presence of a peak at 1657 cm^{-1} is generally associated with the triple helical structure, in line with the commercial type I collagen sample, indicating that both extracted collagen samples have a structure consistent with the hierarchical structure of native collagen.

The presence of amide II, related to N-H bending associated with C-N stretching, is observed from the peak at ~1550 cm^{-1}. Similarly to the Amide I band, the Amide II region has been used to describe collagen structure [29]. The second derivative of the Amide II revealed that commercial type I collagen presents a pronounced peak at 1550 cm^{-1}, indicative of helical structure, absent in the commercial gelatin from fish skin. Both dialyzed collagen and collagen aerogel samples presented one peak at 1549 cm^{-1}, suggesting the presence of a collagen triple helical structure.

The FTIR results indicate that collagen tertiary structure was present in the collagen-NADES extract used for the aerogel production, and the analysis of the collagen aerogel revealed that the developed process did not damage the collagen triple helix.

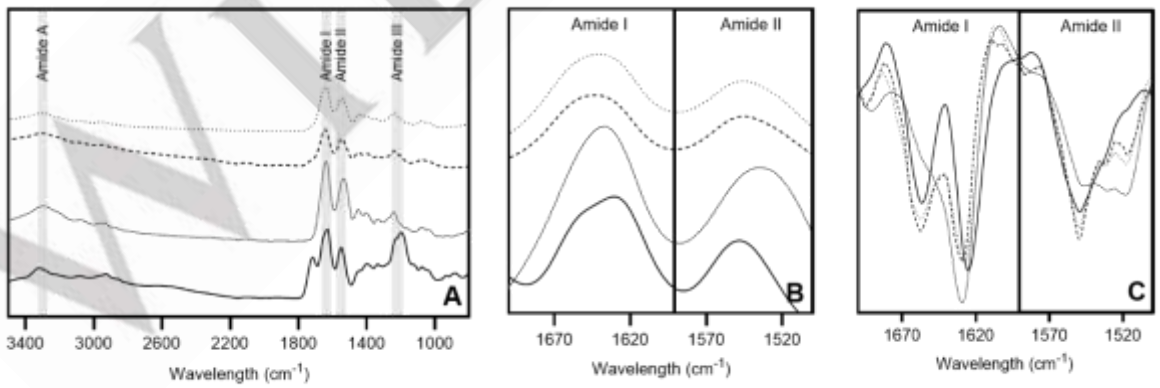

Figure 5. FTIR absorbance spectra of commercial type I collagen from calf skin (—), commercial gelatin from fish skin (—), dialyzed extracted collagen (----), and aerogel processed via direct SE (·····), with the main vibrations of collagen molecular organization, amide A, amide I, amide II, and amide III, highlighted in grey (A); detailed absorbance spectra of Amide I and II bands and their relative second derivatives (B and C, respectively).

Circular dichroism (CD) is another interesting tool for assessing how the aerogel production process affects the collagen triple helical structure. The CD spectra of dialyzed collagen and collagen aerogel were measured and compared to commercial type I collagen and gelatin standards. This analytical technique is used to determine whether the protein exhibits a well-defined CD transition with a positive peak at 222 nm, which indicates the presence of the collagen triple helix [28]. Figure 6 shows CD spectra analysis. All samples presented a negative peak in the 199 nm region. Nonetheless, unlike the commercial native collagen, gelatin did not present a positive peak in the 222 nm region, typical of the tertiary structure. This result agrees with previous reports, where gelatin is the irreversible thermally denatured collagen form composed of random coil structures [27,28]. In turn, dialyzed collagen and collagen aerogel CD spectra showed a positive peak in the 222 nm region, suggesting a triple helix conformation before and after the aerogel production process. Summarizing, CD-spectroscopy and FTIR methodology results consistently show that the aerogel production process did not damage the collagen's initial structure.

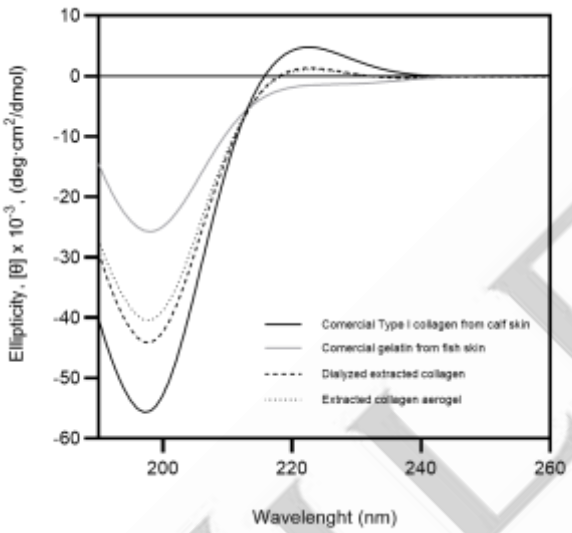

Figure 6. CD spectra of commercial and extracted collagen materials.

Water uptake is an essential parameter in the characterization of protein aerogels, which affects the degradation profile and swelling, inducing changes in mechanical properties and influencing the biological response [24,31]. For topical biomedical applications, the material would benefit from the ability to uptake fluids and remain stable in contact with liquid media at different pH values, from the weakly acidic pH of healthy skin to the slightly basic pH of the wound microenvironment [32]. A water uptake study was performed with the aerogels immersed in phosphate-buffered saline (PBS) at different pH values (4, 7, and 10) at body temperature, and weight increase was recorded for up to 15 days. Collagen aerogels showed a maximum of 2699±217.6 wt% water uptake after 3 days immersed under PBS with a pH of 4. After the third day, the substrate started to lose weight drastically under pH 4, while at pH 10, the collagen aerogel remained at a stable weight for up to 15 days. Tests under neutral pH showed a behavior between pH 4 and pH 10, with lower uptake capacity than pH 4 and remaining stable for 4 days. Collagen aerogels showed higher swelling behavior under neutral pH but lower stability compared to immersion under PBS with a pH of 10. Those were expected results since the aerogels tested are composed of acid-soluble collagen. Therefore, the material typically presents higher water uptake capacity under acid conditions but much higher stability under basic pH. Collagen-based aerogel materials referred to in the literature show water uptake in the wide range from ~100 to ~4000 wt% [10,12,14]. However, besides collagen, these materials contain other polymeric compounds and were prepared by freeze-drying technique; therefore, they are not directly comparable to the matrices prepared in this study. Nevertheless, the aerogels reported in this work demonstrate the water uptake close to the upper bound of this interval. The ability to uptake water and higher stability can be attributed to finer mesoporous structures, which cannot typically be obtained via freeze drying. When exposed to liquid media, aerogels are less susceptible to collapse or deformation, as the smaller pore sizes limit the liquid penetration rate into the material's structure. The increased surface area and pore volume allow longer liquid interaction and higher water uptake capacity. In contrast, freeze-dried macroporous gels tend to collapse quickly in aqueous solutions, due to faster liquid penetration rate [24].

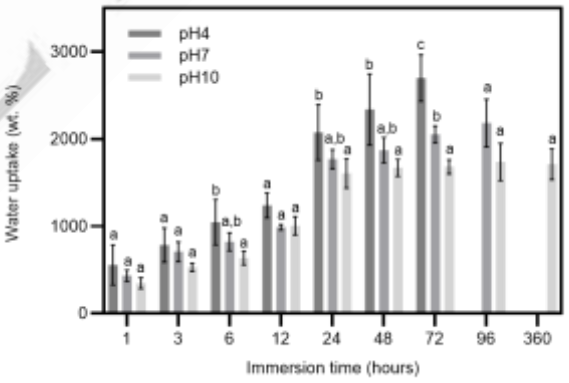

Figure 7. Water uptake of direct SE collagen aerogels under PBS buffer solutions adjusted to different pH. Data are presented as means ± SD of three independent experiments. Bars sharing letters for each time point are not significantly different.

Conclusion

Collagen aerogels were prepared by supercritical drying of alcogels obtained by different SE approaches of a collagen-NADES gelled extract. All obtained aerogels were characterized using microscopy and textural analysis, revealing a mesoporous network structure with a high specific surface area and pore volume. The aerogel obtained by direct SE with methanol

presented as the best candidate for future scale-up and industrial processes. This work simultaneously evaluated the collagen protein integrity after being submitted to the aerogel production process. Collagen in the aerogel was compared with the initial collagen extract while using commercial collagen as a standard. Electrophoretic and two different and complementary spectroscopy characterization techniques revealed no significant impact of the aerogel production process on collagen quality. This work demonstrates the feasibility of an aerogel production process to prepare collagen aerogel materials, ensuring the preservation of the initial tertiary structure of the protein. Water uptake tests showed a high water uptake capacity of up to ~2700 wt.% and a pH-dependent swelling and stability behavior, revealing tunable properties for potential topical biomedical applications. Taken together, the results from this work suggest that this novel aerogel composed of biocompatible marine collagen could be a promising candidate for topical biomedical applications. Future works exploiting the high porosity of these materials for the incorporation of drugs and other bioactive compounds could expand their suitability for topical biomedical applications such as wound healing or drug delivery systems.

Experimental Section

Materials

Absolute ethanol (≥99.8%) and anhydrous pure methanol (>99.8%) were purchased from Fisher Chemical (USA). Food-grade carbon dioxide used for drying was obtained from Air Liquide Portugal (Portugal). Acetic acid (99.7%) was purchased from Panreac (Germany). Commercial Type I collagen from calf skin, commercial gelatin from cold water fish skin, β-mercaptoethanol, and PBS were supplied by Sigma-Aldrich (USA). The protein ladder Precision Plus Protein™ All Blue Prestained Protein Standard, Laemmli Sample Buffer, Tris/Glycine/SDS Running Buffer, and Bio-Safe™ Coomassie Stain were purchased from Bio-Rad (USA).

Aerogels preparation

The collagen aerogels were prepared from the collagen-NADES extract obtained according to the work of Batista et al. [21]. After extraction, the extract was left at 4 ºC for 18 h, getting a gel composed of collagen (0.4 wt.%) and NADES compounds (citric acid:xylitol:water 1:1:10 mol ratio) used for different SE approaches. The SE process was performed by consecutive immersion of the gels in anhydrous pure methanol (at (i) 4 ºC and (ii) -20 ºC) or in methanol/water mixtures (25, 50, 75, and 100 vol%, at 4ºC) until reaching a > 98 vol% methanol content in the supernatant, monitored after each step by a density-meter DMA 4500 (Anton Paar Company, Austria). A final SE step with anhydrous pure methanol was repeated twice before the supercritical drying of alcogels. Finally, the alcogels were dried with $scCO_2$ using high-pressure laboratory equipment (Thar Technology, Pittsburgh, PA, USA, model SFE-500F-2-C50). The drying vessel was preheated to 40 ºC. The vessel loaded with alcogels was pressurized with CO_2 until the desired working conditions (120 bar, 40 ºC) were reached. The CO_2 flow rate was maintained at 90 g/min, and the drying lasted 3 h. All aerogel samples were prepared in duplicates. The main process conditions are summarized in Table 2.

Table 2. Main step conditions of the collagen aerogel production process summarizing the different SE approaches.

Gelation	Solvent exchange (MeOH vol%)	$scCO_2$ drying
4 ºC 18 h	Direct SE (100 vol%), 4 ºC	120 bar 40 ºC 90 g CO_2/min 3 h
	Cryo SE (100 vol%), -20 ºC	
	Stepwise SE (25, 50, 75, and 100 vol%), 4 ºC	

Solid-state characterization

Field emission gun scanning electron microscopy (FEG-SEM)

The morphology of the samples was analyzed using field emission gun scanning electron microscopy (Tescan Mira 3 FEG-SEM) at an accelerating voltage of 5 kV and working distances in the range of 4–6 mm. Before the FEG-SEM analysis, aerogels were sputtered with a thin layer of gold (~7 nm).

Specific surface area and pore volume

Specific surface area, pore volume, and pore diameter were estimated by low-temperature nitrogen adsorption-desorption analysis (Quantachrome Nova 3000e) using BET and BJH methods, respectively. Before the measurements, the samples were degassed at 75 ºC for 24 h.

Physico-chemical characterization

TGA

TGA analysis was performed in a Thermal Analysis instrument (Labsys EVO, Setaram, Caluire, France) in an argon atmosphere, within a temperature range between 25 ºC and 700 ºC with a 10 ºC/min heat ramp.

SDS-PAGE

To evaluate the molecular weight of the obtained protein aerogels, a Bio-Rad Mini-PROTEAN® system (Bio-Rad, USA) was employed to separate proteins by SDS-PAGE. The samples were dissolved in 0.5 M acetic acid (2 mg/mL), mixed in a 1:1 (v:v) dilution with Laemmi sample buffer containing 5% (v/v) β-mercaptoethanol and heated for 10 min at 70 ºC to denature the proteins. The 7.5% Mini-PROTEAN® TGX™ Precast Protein Gel (12-well, 20 µl) was loaded with 10 µL protein ladder and 10 µL from each collagen sample. The samples were run at 200 V for 30 min, and the gel was then stained using the Coomassie stain for 1 h with continuous stirring. Finally, the gel was detained in distilled water overnight and imaged using an iBright FL1500 imaging system software version 1.8.

FTIR spectroscopy

FTIR spectroscopy in attenuated total reflectance (ATR) mode was performed with a Bruker Optics FTIR spectrometer (Bruker IFS 66/S). The presence of collagen's characteristic chemical bonds/groups was evaluated by recording 64 scans between 4,000-650 cm^{-1} with a resolution of 2 cm^{-1}. Using Bruker software OPUS version 6.5, all spectra were ATR-corrected and vector-normalized across the spectrum. Second-derivative spectra were calculated to better separate overlapping absorption bands within the Amide I and Amide II bands (1700–1500 cm^{-1}).

Protein conformation

CD spectra of aerogels were recorded from 190 nm to 260 nm on a Chirascan™ qCD spectrometer/SX20 (Applied Photophysics, UK) using a 0.1 cm^{-1} path length cuvette. Dried samples were dissolved at 1 mg/mL in 0.5 M acetic acid. Samples were loaded at 4 ºC into precooled CD cuvettes.

Water uptake

Dried samples were placed in PBS with different pH values (4, 7, and 10), adjusted using hydrochloric acid or sodium hydroxide, at 37 ºC. The swollen samples were taken out at regular time intervals, wiped superficially with filter paper to remove the surface water, weighed, and placed back in the same PBS bath. The mass measurements were continued until the gels registered a decrease in swelling percentage. The water uptake percentage was determined using the following equation:

$$\text{Water uptake } (\%) = \frac{M_t - M_0}{M_0} \times 100\%,$$

where M_0 and M_t are the initial mass and mass at time t, respectively Mass losses due to disintegration of the swollen samples were not considered in M_t, representing only the water uptake percentage of the undissolved fraction. All the experiments were carried out with three samples, and all data are expressed as mean ± standard deviation (SD). The statistical analysis of the data was performed using GraphPad Prism 9 (GraphPad Software, Inc., CA). All values were tested for normal distribution and equal variance. When homogeneous variances were confirmed, data were analyzed by One Way Analysis of Variance (ANOVA) coupled with Tukey's post hoc analysis to identify means with significant differences.

Acknowledgements

The authors acknowledge the financial support received from the INTERFACE Programme through the Innovation, Technology and Circular Economy Fund (FITEC). iNOVA4Health – UIDB/04462/2020 and UIDP/04462/2020, a program financially supported by Fundação para a Ciência e Tecnologia / Ministério da Ciência, Tecnologia e Ensino Superior, through national funds are acknowledged. Financial support received from The Associate Laboratory LS4FUTURE supported by Fundação para a Ciência e a Tecnologia (FCT, Portugal) through the funding LA/P/0087/2020 (DOI 10.54499/LA/P/0087/2020) are acknowledged. This work also received funding from the ERC-2016-CoG 725034 and was supported by the Associate Laboratory for Green Chemistry (LAQV), financed by national funds from FCT/MCTES (UIDB/50006/2020). The authors acknowledge the financial support received from the Cooperação Cientifica e Tecnologica FCT/DAAD, 2019/2020. Baldur Schroeter acknowledges financial funding through the FMTHH 04FMTHH21 grant. Miguel P. Batista acknowledges FCT for the financial support through the 2020.05895.BD grant. Graphical abstract created with BioRender.com.

Keywords: Porous biomaterials • Collagen tertiary structure • Supercritical CO_2 drying • Solid-state and physicochemical characterization

[1] M. Meyer, *Biomed Eng Online* **2019**, *18*, 1–74.
[2] M. D. Shoulders, R. T. Raines, *Annu Rev Biochem* **2009**, *78*, 929–958.
[3] K. Lin, D. Zhang, M. H. Macedo, W. Cui, B. Sarmento, G. Shen, *Adv Funct Mater* **2019**, *29*, 1–16.
[4] I. Smirnova, P. Gurikov, *Journal of Supercritical Fluids* **2018**, *134*, 228–233.
[5] I. Smirnova, P. Gurikov, *Annu Rev Chem Biomol Eng* **2017**, *8*, 307–334.
[6] H. Maleki, L. Durães, C. A. García-González, P. del Gaudio, A. Portugal, M. Mahmoudi, *Adv Colloid Interface Sci* **2016**, *236*, 1–27.
[7] J. Stergar, U. Maver, *Journal of Sol-Gel Science and Technology 2016 77:3* **2016**, *77*, 738–752.
[8] A. Muñoz-Ruíz, D. M. Escobar-García, M. Quintana, A. Pozos-Guillén, H. Flores, *J Nanomater* **2019**, *2019*, DOI 10.1155/2019/2875375.
[9] B. T. Mekonnen, M. Ragothaman, C. Kalirajan, T. Palanisamy, *RSC Adv* **2016**, *6*, 63071–63077.
[10] D. Govindarajan, N. Duraipandy, K. V. Srivatsan, R. Lakra, P. S. Korapatti, R. Jayavel, M. S. Kiran, *ACS Appl Mater Interfaces* **2017**, *9*, 16939–16950.
[11] F. Zhang, C. Wang, C. Mu, W. Lin, *Polymer (Guildf)* **2022**, *238*, 124402.
[12] G. Dharunya, N. Duraipandy, R. Lakra, P. S. Korapatti, R. Jayavel, M. S. Kiran, *Biomedical Materials (Bristol)* **2016**, *11*, 45011.
[13] L. Baia, M. Baia, V. Danciu, M. G. Albu, V. Coşoveanu, D. Iordăchescu, V. Trandafir, *Journal of Optoelectronics and Advanced Materials* **2008**, *10*, 933–936.
[14] L. Jing, S. Yang, X. Li, Y. Jiang, J. Lou, Z. Liu, Q. Ding, W. Han, *Ind Crops Prod* **2022**, *182*, 114882.
[15] M. Yu, Y. Han, J. Li, L. Wang, *Int J Biol Macromol* **2018**, *115*, 185–193.
[16] R. Wang, P. Zhao, R. Yu, J. Jiang, R. Liang, G. Liu, *Sep Purif Technol* **2022**, *303*, 122209.
[17] S. Liu, C. Zhou, S. Mou, J. Li, M. Zhou, Y. Zeng, C. Luo, J. Sun, Z. Wang, W. Xu, *Materials Science and Engineering C* **2019**, *105*, 110137.
[18] T. Lu, Q. Li, W. Chen, H. Yu, *Compos Sci Technol* **2014**, *94*, 132–138.
[19] W. Zhang, Z. Pan, J. Ma, L. Wei, Z. Chen, J. Wang, *ACS Sustain Chem Eng* **2022**, *10*, 1408–1418.
[20] W. Zhang, Z. Pan, J. Ma, L. Wei, Z. Chen, J. Wang, *ACS Sustain Chem Eng* **2022**, *10*, 1408–1418.
[21] M. P. Batista, N. Fernández, F. B. Gaspar, M. do R. Bronze, A. R. C. Duarte, *Front Chem* **2022**, *10*, 1–10.
[22] M. E. El-Naggar, S. I. Othman, A. A. Allam, O. M. Morsy, *Int J Biol Macromol* **2020**, *145*, 1115–1128.
[23] P. Selvasekaran, R. Chidambaram, *Trends Food Sci Technol* **2021**, *112*, 455–470.
[24] M. Betz, C. A. García-González, R. P. Subrahmanyam, I. Smirnova, U. Kulozik, *J Supercrit Fluids* **2012**, *72*, 111–119.
[25] S. Zhao, W. J. Malfait, N. Guerrero-Alburquerque, M. M. Koebel, G. Nyström, *Angewandte Chemie - International Edition* **2018**, *57*, 7580–7608.
[26] J. Rouquerol, G. V. Baron, R. Denoyel, H. Giesche, J. Groen, P. Klobes, P. Levitz, A. V. Neimark, S. Rigby, R. Skudas, K. Sing, M. Thommes, K. Unger, *Microporous and Mesoporous Materials* **2012**, *154*, 2–6.
[27] A. M. Carvalho, A. P. Marques, T. H. Silva, R. L. Reis, *Mar Drugs* **2018**, *16*, 1–14.
[28] H. Jafari, A. Lista, M. M. Siekapen, P. Ghaffari-Bohlouli, L. Nie, H. Alimoradi, A. Shavandi, *Polymers (Basel)* **2020**, *12*, 1–37.
[29] K. H. Sizeland, K. A. Hofman, I. C. Hallett, D. E. Martin, J. Potgieter, N. M. Kirby, A. Hawley, S. T. Mudie, T. M. Ryan, R. G. Haverkamp, M. H. Cumming, *Materialia (Oxf)* **2018**, *3*, 90–96.

10.1002/cplu.202400122

[30] C. Stani, L. Vaccari, E. Mitri, G. Birarda, *Spectrochim Acta A Mol Biomol Spectrosc* **2020**, *229*, 118006.
[31] S. Groult, S. Buwalda, T. Budtova, *Materials Science and Engineering: C* **2021**, *126*, 112148.
[32] P. C. Pires, F. Mascarenhas-Melo, K. Pedrosa, D. Lopes, J. Lopes, A. Macário-Soares, D. Peixoto, P. S. Giram, F. Veiga, A. C. Paiva-Santos, *Eur Polym J* **2023**, *187*, 111868.

10.1002/cplu.202400122

WILEY VCH

RESEARCH ARTICLE

Entry for the Table of Contents

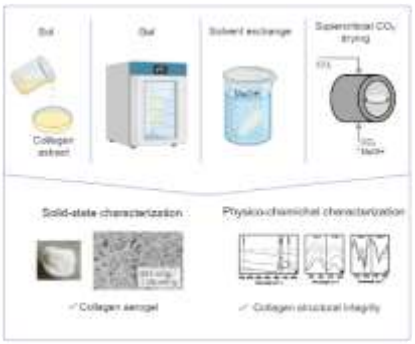

The study investigated the production of a novel collagen aerogel obtained through solvent exchange and supercritical CO_2 drying of a gelled marine collagen extract for potential topical biomedical applications. Morphology and textural analysis confirmed the obtention of a novel collagen aerogel, and physicochemical analysis revealed no impact of the aerogel production process on collagen tertiary structure.

Institute and/or researcher Twitter usernames:

@ibetportugal